The Meteoritical Society

Meteoritics & Planetary Science 42, Nr 4/5, 635–654 (2007)
Abstract available online at http://meteoritics.org

The ICDP Lake Bosumtwi impact crater scientific drilling project (Ghana): Core LB-08A litho-log, related ejecta, and shock recovery experiments

Alexander DEUTSCH*, Sabine LUETKE, and Volker HEINRICH

Institut für Planetologie, Westfälische Wilhelms-Universität Münster, Wilhelm-Klemm-Str. 10, D-48149 Münster, Germany
*Corresponding author. E-mail: deutsca@uni-muenster.de

(Received 07 September 2006; revision accepted 23 December 2006)

Abstract–The 1.07 Myr old Lake Bosumtwi impact crater in Ghana was drilled within the framework of the International Continental Scientific Drilling Project (ICDP). Hole LB-08A, drilled into the outer flank of the central uplift and with a total depth of 451 m, yielded 215.71 m of impact-related rocks. This paper summarizes observations of the lithological logging on core LB-08A. Between a depth of 235.6 and ~260 m, the section consists of a melt-bearing allochthonous, polymict, and mostly clast-supported impact breccia. Down to ~418 m, the section comprises a rather uniform unit of meta-graywacke alternating with phyllite to slate (lower greenschist facies); few (par-) autochthonous impact breccia bodies and rare impact dike breccias are present. The lowermost part of the section contains several centimeter- to decimeter-thick melt-bearing breccia dikes in country rocks identical to those occurring above. Omnipresent fracturing was mapped in a qualitative manner. Most prominent shock effects in the uplifted target rocks comprise planar fractures and deformation elements in quartz and polysynthetic twinning in carbonate minerals; the maximum shock pressure as evidenced by quartz is below 26 GPa. The allochthonous breccias occasionally contain a few vol% of melt particles. Suevites occur outside the crater rim, carrying diaplectic crystals, coesite, and ballen quartz as well as true melt glasses and a variety of lithic clasts, among those spectacular staurolite-rich mica-schists. The recorded shock level in the uplifted target rocks is lower than expected and modeled. Shock recovery experiments with analogue carbonaceous graywackes at 34 and 39.5 GPa yielded nearly complete transformation of quartz into diaplectic glass. We therefore exclude a specific shock behavior of the soft, fluid-rich target material (carbonaceous graywackes, shales, slates) in core LB-08A as the prime or only reason for the melt deficit and the generally low shock levels recorded inside the Lake Bosumtwi impact crater.

INTRODUCTION

The Lake Bosumtwi impact structure, centered at 6°30′N, 1°25′W, is located in the southern rain forest of Ghana, West Africa (Fig. 1), roughly 32 km southeast of Kumasi, the capital of the Ashanti region. The crater has a rim-to-rim diameter of ~10.5 km and a subdued elevation feature at a distance of ~10 to 11 km from the crater center (Wagner et al. 2002). The crater is filled by Lake Bosumtwi, which is up to 81 m deep and has a diameter of ~8 km. Due to its young age of only 1.07 Myr (Koeberl et al. 1997), the crater is excellently preserved. Moreover, it is most likely the source of the Ivory Coast tektites and the associated microtektites found in the deep-sea drill cores in the Atlantic Ocean (e.g., Glass et al. 1991; Koeberl et al. 1997) (insert in Fig. 1). The Lake Bosumtwi structure therefore provides an exceptional example for general analysis of medium-sized terrestrial impact craters.

Target rocks in the Bosumtwi area are mainly Proterozoic metasediments, namely graywackes, carbon-rich phyllites, schists, and quartzites, and subordinately metavolcanics of the approximately 2.1 Gyr old Birimian Supergroup. Coarse clastic sedimentary rocks of the slightly younger Tarkwaian Supergroup occur to the southeast of the crater (Fig. 1). Some syndeformational granitic intrusions that include a variety of other rock types (e.g., hornblende diorite, two mica granite) and granitic dikes crop out around the north, west, and south sides of Lake Bosumtwi (for a review, see Koeberl and Reimold 2005).

Recent refraction and reflection seismic surveys (Karp et al. 2002; Scholz et al. 2002; Danuor 2004; Ugalde 2006; Ugalde et al. 2007) (see traces of the seismic lines in Fig. 1)

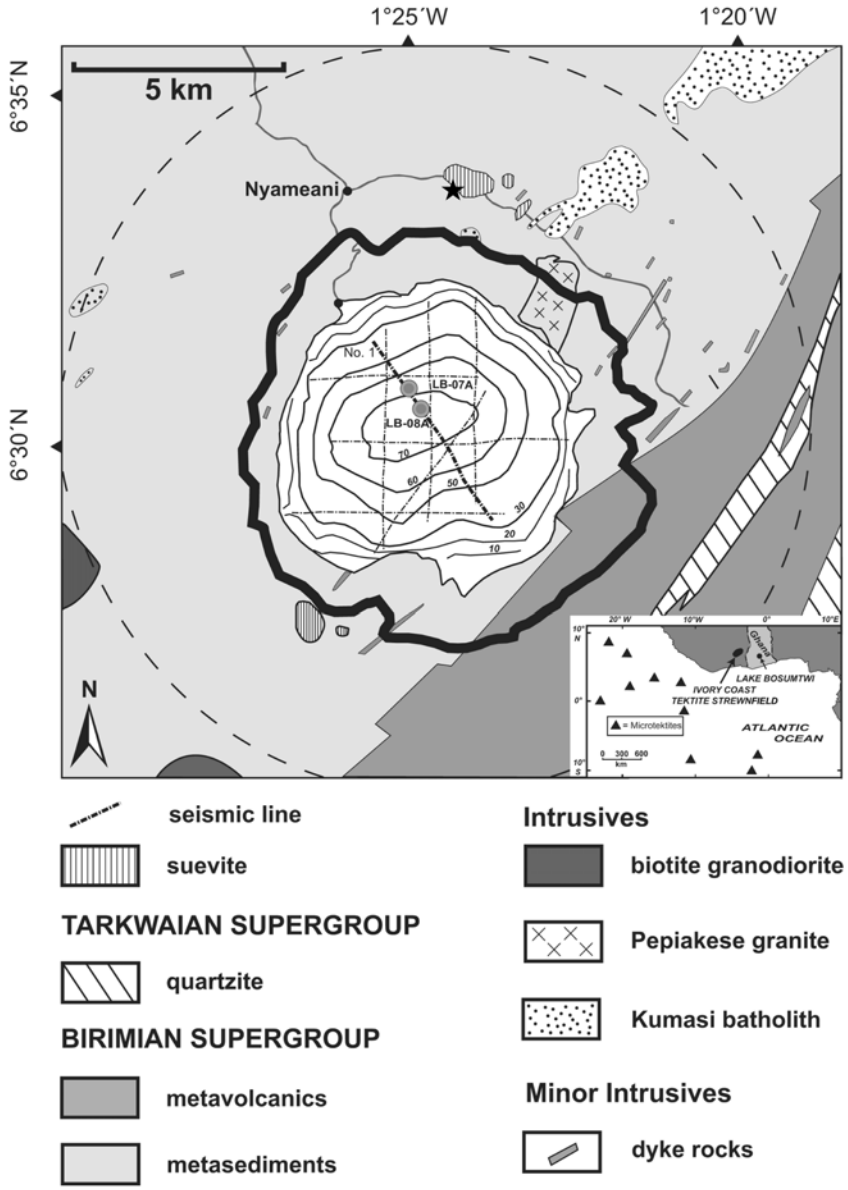

Fig. 1. A geological sketch map of the Lake Bosumtwi impact structure, Ghana, including lake shore and bathymetry, locations of the reflection seismic profiles acquired in 1997, the "hard-rock" drill sites, LB-07A and LB-08A, and the sampling location for suevite (★). The figure was compiled from the revised geological map 1:50,000 (Geological Survey of Austria; Koeberl and Reimold 2005), and Fig. 6.8 of Ugalde (2006). Figure 2 shows the profile along seismic line no. 1, on which LB-07A and LB-08A were drilled. The dark line corresponds to the morphological crater rim; the dashed line marks the approximate position of the outer topographic ring (Wagner et al. 2002). The lake has a mean depth of 45 m. The maximum depth encountered in 2004 was 74 m; bathymetric contours are in meters. The insert shows the location of Lake Bosumtwi, the Ivory Coast tektite strewn field, and the microtektite-bearing drill cores (U.S. Navy, Lamont-Doherty Earth Observatory, and Ocean Drilling Program cores). Insert modified after Koeberl et al. (1997).

and airborne high-resolution total magnetic field, electromagnetic field, and gamma radiation measurements (Plado et al. 2000; Pesonen et al. 2003) helped to resolve the subsurface structure of the Bosumtwi crater in great detail (Fig. 2). The interpreted data were used to predict very precisely the boundary between post-impact lake sediments and impact-related features such as the ~1.8 km wide central peak, which surmounts the top of the breccia in the annular moat by about 120 m (e.g., Scholz et al. 2002) (Fig. 2). Based on these detailed geophysical data, Karp et al. (2002) and Artemieva et al. (2004) modeled various possible impact conditions; moreover, these authors made predictions on impact-related rock formations below the lacustrine post-impact sediments, whose thickness was precisely assessed by seismic methods to amount to between ~50 and 310 m. Beneath these sediments, seismic survey data revealed an

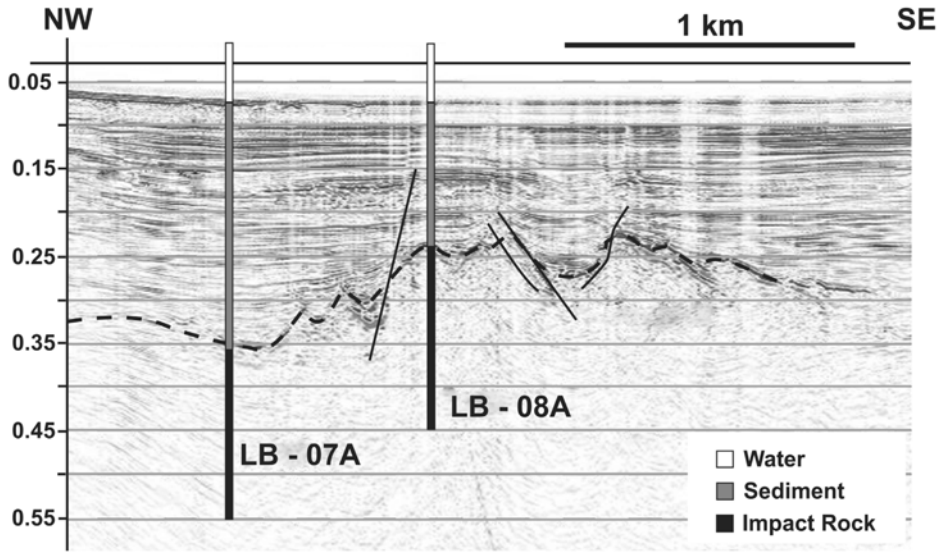

Fig. 2. Vertically exaggerated (1:3) schematic reflection seismic profile with the locations of "hard rock" drill sites LB-07A and LB-08A. Note the precise definition of the top of the impact-related structural features, the central peak and annular moat. Some internal structures including faults are readily identifiable, yet the base of these features is not visible. Modified after Scholz et al. (2002).

intermediate velocity layer (3200 m s^{-1}) (Fig. 2) interpreted to represent either fallback breccia or a breccia/impact-melt rock formation (e.g., Karp et al. 2002). Models on the basis of low-altitude airborne magnetic data strongly supported the presence of impact-melt rock or melt-rich suevite bodies beneath the post-impact cover (Plado et al. 2000; Pesonen et al. 2003).

Lake Bosumtwi was selected as the target for the International Continental Scientific Drilling Project (ICDP). The paleo-environmental rationale for the Lake Bosumtwi Impact Crater Drilling Project (BCDP) was the presence of a complete 1 Myr old climate archive in the intertropical convergence zone, which in West Africa is a region with a very sparse continuous sedimentological record (Koeberl et al. 2007). One major goal of the drilling campaign was therefore to collect several complete sections of the lacustrine sediments (Fig. 2) to get a detailed understanding of long-term monsoon variations in West Africa. The Lake Bosumtwi structure offers the possibility of studying in detail the subsurface structure with geophysical methods (see above), and, with the help of drilling, correlating geophysical and modeling results with borehole logs and petrological and petrophysical data on core samples.

Actual ICDP drilling, coring, borehole logging, and additional geophysical surveys were performed between July and October 2004 (Koeberl et al. 2007). At five sites, 14 separate holes were drilled into the lake sediments; total recovery was 1833 m. Two BCDP well holes were designed to core "impact-related hard rocks," namely LB-07A (total hole depth of 548 m, casing from 69 to 332 m depth; total core 217.42 m in 49 core boxes, each containing approximately three meters of core, and stored at ICDP facilities, GeoForschungsZentrum, Potsdam, Germany [GFZ]) into the annular moat, and LB-08A (total depth of 451 m; casing from 64 to 235.61 m; total core 215.71 m in 73 core boxes [Figs. 3 and 4]) into the outer flank of the central uplift (Figs. 1 and 2).

Here we provide a comprehensive lithological description of core LB-08A, based on a three-week core logging session (http://www.icdp-online.de/contenido/icdp/upload/pdf/lake_bosumtwi/secure/lithounits_8A.txt) at the GFZ. The detailed original logs are available on request from the senior author. In addition, we discuss the shock metamorphic overprint of rocks in this core and provide results of the experimental validation of the shock assessment. Another lithological description for core LB-08A is provided by Ferrière et al. (2007a); Coney et al. (2007a) describe the lithoprofile and shock metamorphism in rocks (Morrow 2007) of core LB-07A.

SAMPLES AND ANALYTICAL TECHNIQUES

For the petrological classification of lithologies in core LB-08A, 71 samples were taken (Fig. 4). Of those, 40 representative thin sections were analyzed by optical microscopy and partly by scanning electron microscope (SEM) (JEOL JS-840 A, 20 kV acceleration voltage; ICEM WWU Münster). Quantitative determination of modal composition was performed on 22 powdered whole-rock samples by X-ray diffraction analyses (XRD) (powder diffractometer PANalytical, X'Pert PW 3040, equipped with a $Cu_{K\alpha 1}$ X-ray radiation source, running at 40 kV, 35 mA, and a solid state or scintillation detector) in the 2 Θ range of 2–50° at a scan rate of one degree/minute using a sample spinner to reduce effects of preferred orientation.

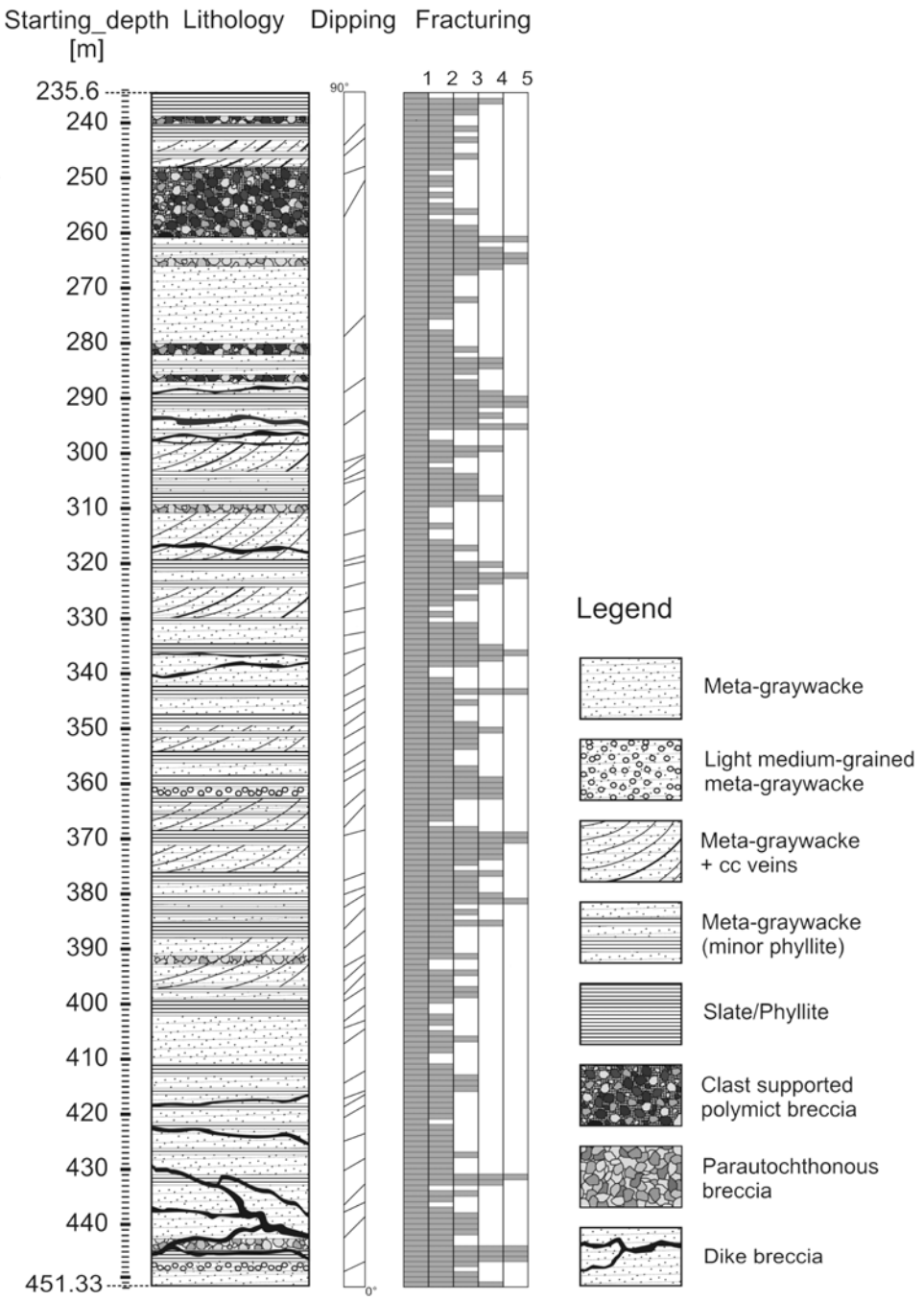

Fig. 3. A schematic lithological profile of core LB-08A illustrating intensity of fracturing and dipping of the lithological units relative to the axis of the core. Classification of fracturing: 1 = insignificant, 5 = total disintegration.

In this work, we use sample labeling as given by the operational support group (OSG) of the ICDP at the GFZ. For example, SR0037B0037-2-285,285 means sample run 37, box 37, row 2, top and bottom distance of the core sample from the beginning of the respective run in centimeters. Figure 4 shows the respective depth of each analyzed core piece. Color names are used according to the rock color chart committee (1979).

SUEVITES AND TARGET LITHOLOGIES OUTSIDE THE MORPHOLOGICAL CRATER RIM

Because weathering in the Bosumtwi area is very intense (cf. Boamah and Koeberl 2002), fresh rocks are exclusively found along road cuts or as large boulders on the outer flank of the crater rim. Following the compilation by Koeberl and Reimold (2005), dominant lithologies are meta-graywackes,

phyllites, and graphitic schists locally intruded by small dikes and pods of granites; fine-grained tuffaceous phyllites and schists are also present. In the Birimian units, breccia occurrences are frequent in the Bosumtwi area, some of which have been assumed to be the product of "secondary mass-wasting processes" (Reimold et al. 1998). Polymict and glass-bearing breccias, however, are unambiguously assigned as impact lithologies; their thickness may reach up to 20 m (Koeberl and Reimold 2005). Our own sampling north off the crater rim (cf. Fig. 1) yielded boulders of i) slates to phyllites, rich in dark organic matter and characterized by orthogonal prisms grown across the well-defined schistosity—such rocks form an important component in the target lithologies drilled in LB-08A; ii) meta-graywackes; iii) meta-tuffites with millimeter-size albite porphyroclasts; iv) two-mica schists; v) spectacular staurolite-rich mica-schists (Figs. 5a and 5b; Deutsch et al. [2005]); vi) highly shocked biotite-gneiss; vii) suevites, containing fragments of the lithologies given above, ballen quartz as well as fresh diaplectic and melt glasses (Figs. 5c and 5d), the latter in part with <10 μm size crystallites; and viii) highly vesicular impact-melt rocks with a crypto- to microcrystalline groundmass; the macroscopic appearance of this rock type resembles a highly shocked gneiss. The occurrence of staurolite as index mineral for amphibolite-facies metamorphism in lower Birimian units has been reported by Moon and Mason (1967), yet the presence of staurolite schists so close to the Bosumtwi crater, and as clasts in suevites, is a new observation. As detailed below, this spectrum of rocks is much broader than that of core LB-08A.

CORE LB-08A

Lithologies

Two major groups of rocks were encountered in LB-08A: target rocks and impact breccias. The post-impact lake sediments were penetrated by rotary drilling and are not considered further in this article. Figure 3 shows a simplified lithological profile of LB-08A.

Target Rocks

Only two principal target lithologies occur in this well, a medium to very light gray (color chart N6 to N8) meta-graywacke (Figs. 6 and 7), and light gray to medium dark gray (N6 to N4), mostly fine laminated phyllites to slates (Fig. 8) with all transitions in between (Fig. 7). Geochemical data, i.e., SiO_2 contents of 50 wt% or less in combination with Ni-carrying sulfides, indicate the presence of metavolcanic target rocks in core LB-07A (Kontny et al. 2007), yet such material is not present in our sample suite of LB-08A. The graywackes and shales form cyclic sedimentary sequences with thicknesses between 20 and 100 cm. In the core, these sequences are overturned, i.e., grain size of the individual components in the metasediments decreases downward. The boundaries between respective sequences are often sharp and disconformable; some core pieces provide evidence for syn- to post-sedimentary offsets due to slumping and/or compaction processes. According to XRD analyses, modal composition of these rocks is quartz, albite, illite to 2T muscovite, (ferroan) clinochlore, and calcite (+ Fe-rich and dolomitic varieties) in various proportions. Minor and trace constituents include epidote-clinozoisite, tourmaline, rutile, zircon, oxides-hydroxides, and sulfides; the latter rarely exceed 1 vol% (Kontny et al. 2007). Finely dispersed inorganic and organic carbonaceous matter is also present.

Meta-graywacke: Meta-graywacke is the dominant lithology among the target rocks in core LB-08A (Figs. 6 and 7). The characteristic spotty appearance (Fig. 6a) is caused by the mineral clasts embedded in a clastic matrix, composed in decreasing order of occurrence by quartz, chlorite, sericite, feldspar, and carbonate minerals. At the microscopic scale, the rocks have a flaser texture (Fig. 6b). In the matrix, lobate intergrowth of the quartz grains is common, explained by pressure solution during diagenesis. The prevailing fragments are quartz, altered albite to oligoclase with partly simple, partly polysynthetic twinning, while lithic clasts and aggregates of organic dark matter occur only in minor amounts. Triple junctions are common (Fig. 6c). Coarser-grained meta-graywackes with clast sizes on the order of some millimeters display a low degree of sorting; the finer-grained variants have a more homogeneous distribution of grain sizes. As shown in Figs. 7b and 7d, these types of meta-graywackes grade into phyllites at distances of a few millimeters. Compared to common meta-graywackes, the samples from LB-08A are very carbonaceous; some contain up to about 20 vol% calcite (dolomite and Fe-rich calcite in minor quantities) at the thin section scale. The high calcite abundance is reflected in CaO contents in excess of 6 wt% (meta-graywackes in LB-07A [Coney et al. 2007b] and LB-08A [Ferrière et al. 2007b]). These carbonates are tightly intergrown with quartz; their origin is unconstrained and may be diagenetic, but is definitely pre-impact, as documented by the ubiquitous presence of shock features (Fig. 6b; see below). Occasionally intraformational shale clasts up to 5 cm in size occur.

A specific type of meta-graywacke (cf. Figs. 3 and 4) are coarse, sandy, medium-light gray rocks with a flaser texture (Fig. 7a), rich in plagioclase clasts (up to 10 mm across), containing in addition some clasts with a "granophyric" intergrowth of quartz and albite (Fig. 7c); the matrix consists again of mica flakes (less than 0.3 mm in length), chlorite (in part grown in rosettes) with anomalous brownish birefringence colors, and calcite. Regarding the whole core, this rock is very prominent due to its light color and its apparently unbrecciated nature. Terms like "granophyric textured rock/vein" or "graywacke containing granophyric material" are also in use for the meta-graywacke. Like the "normal" meta-graywackes, however, this light gray variety is also a clastic sediment, possibly with a slightly different source rock.

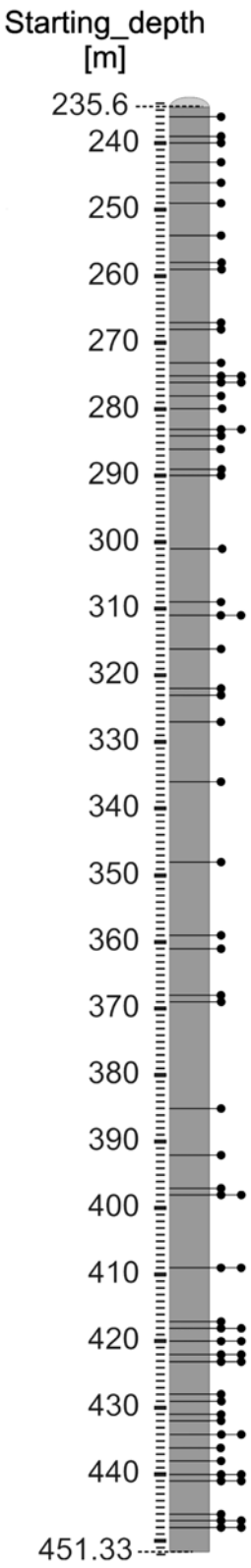

Run	Sample name	Starting_depth [m]	Lithology
01	B0001-1-20,26	235.85	ibr (polymict)
02	B0001-4-37,40	239.02	ibr (polymict)
	B0002-1-129,134	239.94	ibr (polymict)
03	B0003-1-120,125	242.90	slate
04	B0005-3-125,130	246.00	ibr (shale)
05	B0005-4-160,165	249.40	ibr (polymict)
07	B0007-2-13,19	254.02	ibr
08	B0008-5-151,157	258.45	ibr (polymict)
	B0009-2-247,252	259.41	ibr
11	B0010-3-40,40	266.48	mgw (fg)
	B0011-1-210,215	268.18	slate
13	B0012-2-316,318	272.62	mgw (fg)
	B0013-1-241,246	274.59	mgw (fg)
	B0013-1-248,248	274.66	mgw (mg)
14	B0013-3-40,45	275.63	mgw (mg)
	B0013-4-160,161	275.70	mgw to slate
	B0014-2-276,276	277.99	mgw (fg)
15	B0015-2-192,196	280.20	ibr (polymict)
16	B0016-1-157,157	282.89	mgw (fg)
	B0016-1-170,175	283.02	mgw (fg)
	B0016-2-218,218	283.50	mgw (fg)
17	B0017-2-170,176	286.07	ibr (polymict)
18	B0017-5-174,174	289.16	mgw (fg)
	B0018-2-298,301	290.40	phyllite
22	B0021-2-169,169	301.30	slate
25	B0024-2-53,53	309.29	mgw (fg)
	B0024-4-182,182	310.58	slate
	B0024-5-240,245	311.16	ibr, monomict
27	B0026-5-122,125	316.07	slate
29	B0028-5-74,74	321.70	mgw (fg)
	B0029-2-167,167	322.62	slate
31	B0030-4-21,21	327.25	slate
33	B0033-3-299,301	335.56	slate
37	B0037-2-285,285	348.18	slate
41	B0041-1-96,96	358.48	mgw (fg)
42	B0042-1-73,73	361.30	l-mgw (fg) "granophyric"
44	B0044-3-105,105	367.72	mgw (fg)
	B0045-1-245,245	369.12	mgw
49	B0049-5-260,265	384.51	mgw (fg)
52	B0052-5-92,92	391.97	mgw (fg)
53	B0054-4-290,295	397.00	slate
54	B0054-5-38,38	397.53	mgw (fg)
	B0055-1-91,91	398.06	slate
57	B0059-1-304,309	409.33	mgw (fg)
58	B0059-2-3,8	409.37	mgw (fg)
60	B0062-1-175,175	417.19	mgw (fg)
	B0062-2-202,202	417.46	mgw (fg)
61	B0062-3-340,348	418.43	mgw (fg)
	B0062-5-108,113	419.56	slate
	B0063-4-283,288	420.00	mgw (fg)
62	B0064-1-78,81	422.31	ibr (polymict)
	B0064-1-84,88	422.37	ibr (dike)
	B0064-1-96,100	422.49	ibr (dike)
	B0064-1-106,110	422.60	mgw (fg)
64	B0066-1-34,39	427.96	phyllite
	B0066-3-156,162	429.19	mgw (mg)
65	B0067-1-5,8	430.75	mgw (fg)
	B0067-3-145,150	432.13	qtz vein
66	B0068-1-80,85	433.52	ibr (polymict)
	B0068-2-70,75	434.42	ibr (dike)
	B0068-2-81,87	434.53	ibr (dike)
67	B0069-3-86,92	437.63	ibr (polymict)
68	B0070-2-14,20	439.96	ibr (dike)
	B0070-3-46,50	440.29	ibr (dike)
	B0070-3-81,85	440.64	ibr (dike)
	B0070-4-91,96	440.90	ibr (dike)
70	B0071-5-19,22	446.11	mgw (mg)
	B0072-1-86,92	446.78	ibr (dike)
	B0072-2-99,105	446.91	l-mgw (mg) "granophyric"
	B0072-3-181,181	447.73	mge (mg)
	B0072-3-200,205	447.92	mgw (fg) + qtz veins

ibr: impact breccia; mgw: meta-graywacke; l-mgw: light meta-graywacke; fg: fine grained; mg: medium grained

Fig. 4. A depth profile of core LB-08A giving the respective position of each sample (—•) used for this work.

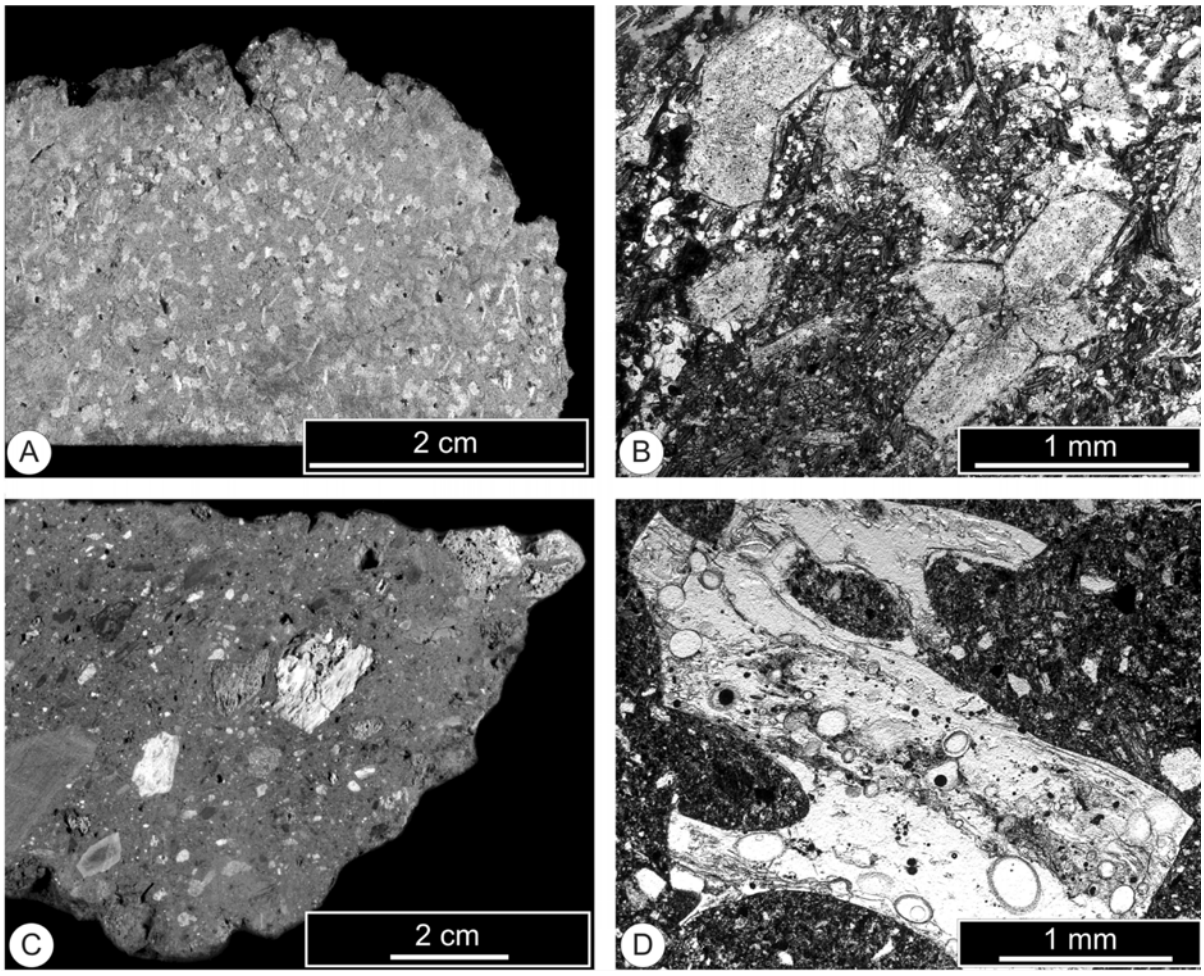

Fig. 5. Impact-related lithologies present at localities south of the unpaved road between Nyameani and Nkowinkwanta (~2.7 km off the northern shore of Lake Bosumtwi, Ghana) (cf. Fig. 1). a, b) Two mica schists with up to 20 vol% sericite pseudomorphs after twinned staurolite crystals. Sample BOT 6. c, d) Glass-rich suevite with a clast population comprising schists, slates rich in organic material, whole-rock melt glass, and mineral fragments, among those quartz melt glass and diaplectic quartz glass with coesite. Sample BOT 12. d) Schlieren-rich melt glass fragment with numerous vesicles/bubbles lined with clay minerals in a clastic matrix consisting of rock fragments and clasts of tectosilicates, chlorite, biotite, and sericite. (a) and (c) are hand-specimens; (b) and (d) are micrographs // nicols.

Phyllites to slates: Phyllites to slates consist of alternating 1–2 mm wide bands of quartz with subordinate calcite and, rarely, albite and quartz (sedimentary) clasts up to 1 mm large, and extremely fine-grained quartz-sheet silicate layers. The quartz grains are less than <0.02 mm across, and 120° triple junctions are common. The less than 1 mm thin bands of quartz-sericite-chlorite-organic matter (<1 mm) occasionally display kinking (Fig. 8a) and folding, onset of shearing, and crenulation cleavage that postdates mineral growth yet predates the shock event. Isoclinal folding is occasionally present as well. Some phyllites contain up to 0.5 wt% finely dispersed organic (e.g., sample SR0037B0037-2-285,285 [cf. Fig. 4]: total organic carbon [TOC] < 0.3 wt%) and inorganic carbonaceous (TIC about 0.2 wt%) matter causing the medium-dark gray color of some bands and layers (Figs. 7d and 8a). Occasionally, nontransparent black clusters (Fig. 8b) or streaks are present; in addition, hypidiomorphic nontransparent prisms grow orthogonal to the fabric (Figs. 8c and 8d). All three features may contain finely dispersed grains or thin veinlets of sulfides (Figs. 8c and 8d). Sulfides also form elongated grains or aggregates parallel to the foliation (Fig. 8c).

Regional-metamorphic overprint: All target lithologies found in LB-08A display a pre-impact regional-metamorphic overprint, which reflects conditions of lower greenschist facies. This metamorphic grade is lower than described for the Birimian sequences in the surroundings of Lake Bosumtwi—they are overprinted in upper to lower amphibolite-facies (e.g., Moon and Mason 1967; Jones et al. 1981; Koeberl et al. 1998; for review see Koeberl and Reimold 2005). Clasts of such metamorphites are totally lacking in the polymict breccias of core LB-08A. They are, however, present in the fallout suevites outside the morphologic rim of the Lake Bosumtwi impact structure.

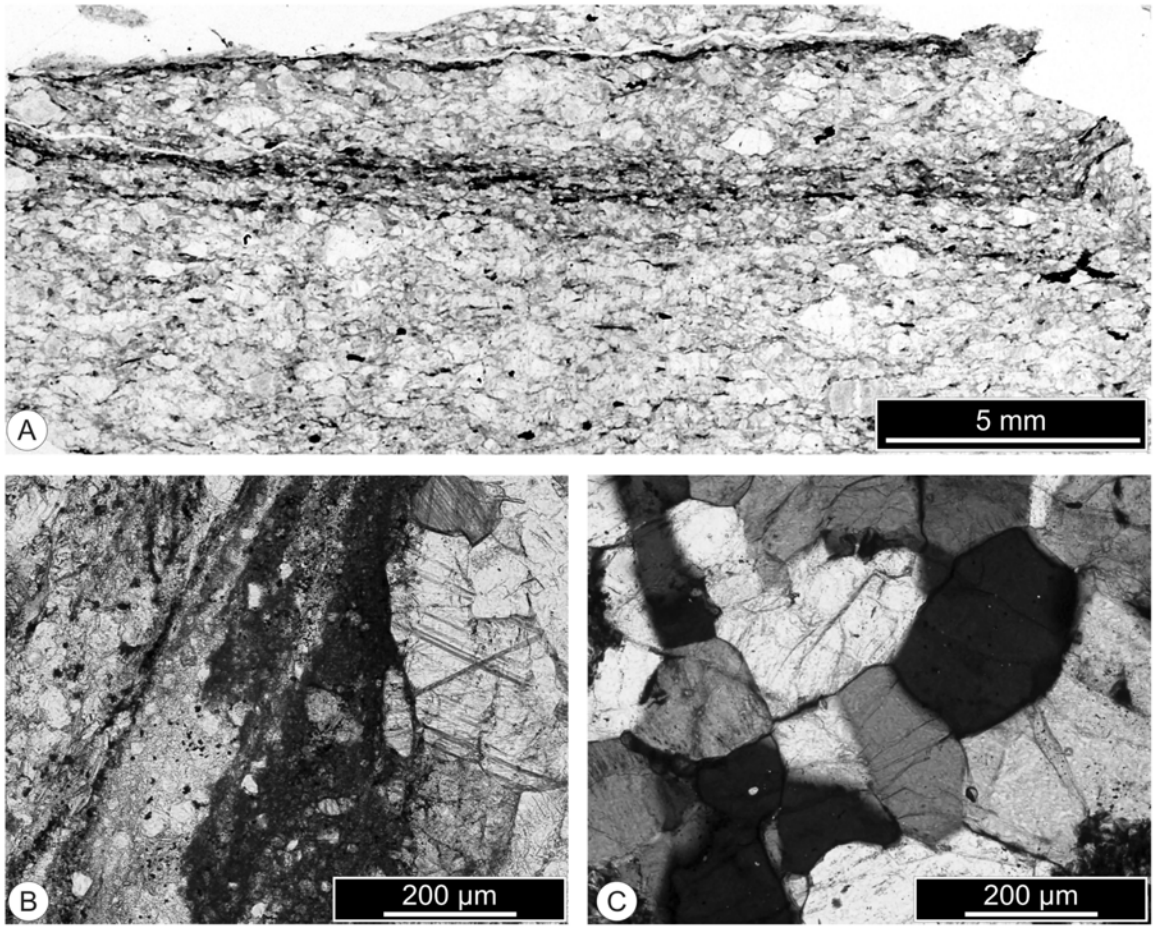

Fig. 6. Micrographs of meta-graywackes in core LB-08A. a) A rather well-sorted typical example with clasts of quartz, partly strongly saussuritized, twinned albite-oligoclase crystals. Calcite is only present in minor amounts. Sample SR0044B0045-1-245,245. b) Calcite forms streaks and seams. Sample SR0042B0042-1-73,73. c) Equant quartz crystals with 120° grain boundaries. Sample SR0011B0010-3-40,40. (a) is a macrophoto of thin section, (b) //, (c) + nicols.

Alteration—pre- or post-impact in age? Using microscopic techniques only, the overall post-impact alteration is not easily assessed. Traces of a (late to post-Birimian?) alteration phase, however, are well documented in most target rocks. They include i) different degrees of saussuritization of the albite to oligoclase crystals; ii) the presence of veins, stringers, and stockworks of quartz and calcite crosscutting layering and schistosity (this generation of veins is always brecciated); and iii) coating of the walls of open (pre-impact) fractures with greenish to greenish gray chlorite and calcite. It is unconstrained if the sporadically found framboidal, ~2 mm size sulfide (pyrite?) aggregates on open fractures are (e.g., at a depth of ~389 m) also a pre-impact feature.

Rusty spots (goethite and hematite) and sulfides on fractures, clay minerals on clast surfaces in breccias, and the alteration of glass fragments to clays clearly belong to a post-impact alteration phase. Kontny et al. (2007) deduced peak shock temperatures on the order of 320 °C for the target lithologies in core LB-08A from the magnetic mineralogy data. According to their investigation, pyrrhotite, the major carrier of the magnetic signal, is a pre-impact phase that was crushed and fractured by the shock. Due to the generally rather low peak shock temperature and the near-total absence of melt lithologies, conditions for generating a long-lasting hydrothermal system were obviously not present in the central peak region of the Lake Bosumtwi crater.

Impact Breccias

This group includes allochthonous and (par-) autochthonous breccias (Figs. 9 and 10).

The allochthonous breccias that are light olive gray (5Y6/1), dark greenish gray (5GY4/1), or olive gray (5Y4/1) are polymict and amount to ~19 m (i.e., 9%) of the totally recovered core. The polymict lithic breccias have a clastic matrix, form compact bodies with diffuse to sharp boundaries to the respective host rocks or fragments (Figs. 9a, 10b–g), and occur in the upper part of the core. There, the overall

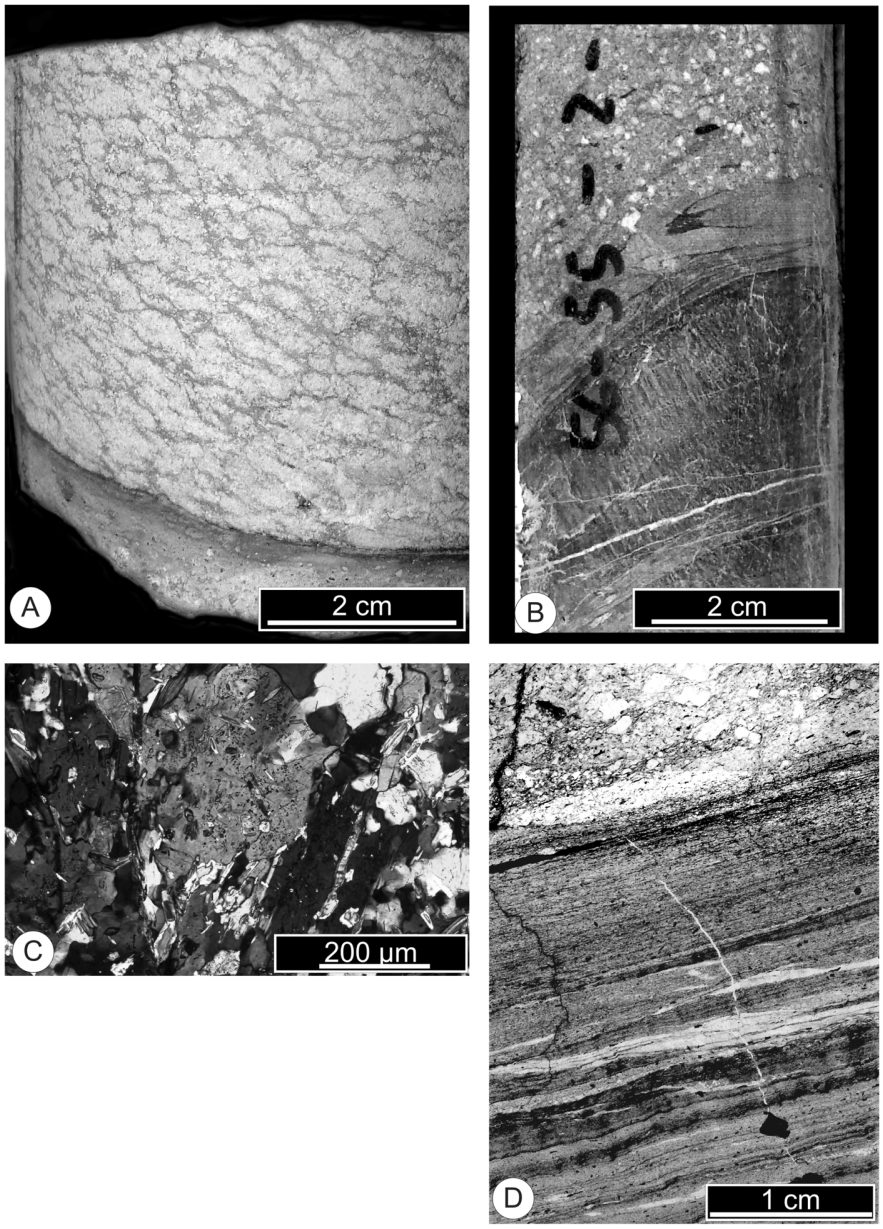

Fig. 7. Meta-graywackes in core LB-08A. a, c) Light, medium to coarse sandy type, containing clasts with a "granophyric" texture. Sample SR0070B0072-2-99;105. b) The meta-graywacke grades in most core intervals from coarse- to medium-grained over fine-grained varieties to phyllite without macroscopically visible clasts. Core piece SR0055B0056-2. c) A clast with an intergrowth of quartz and albite with sericite flakes ("granophyric intergrowth;" see text) in a finer-grained matrix consisting of quartz, albite, chlorite, and sericite. Sample SR0042B0042-1-73,73. d) Smooth transition from meta-graywacke to banded and strongly foliated phyllite. The dark irregular "tetragonal" aggregate is enlarged in Fig. 8b. Sample SR0053B0054-4-290,295. (a) and (b) are macrophotos (half core), (c) is a micrograph with + nicols, (d) is a macrophoto of thin section.

appearance is that of a clast-supported texture. Dike breccias, also belonging to the group of allochthonous breccias, are between a few and a few tens of centimeters thick and form branching systems (Fig. 3), crosscutting the host rocks always with sharp boundaries (Fig. 9b). Occasionally the marginal zone displays brownish colors and resembles the selvedge of an igneous dike, and a rather blurred flow texture may be present.

Both types of allochthonous breccias carry clasts of directly adjacent host rocks as well as exotic clasts. The latter one includes "granophyric-textured" grains (cf. Fig. 7c), extremely fine-grained slates, and opaque material (Fig. 10f), presumably slates with organic matter. These rock types, however, are exclusively those that occur elsewhere in the LB-08A core. Higher metamorphic schists or granites as mapped at or just outside the crater rim or occurring as

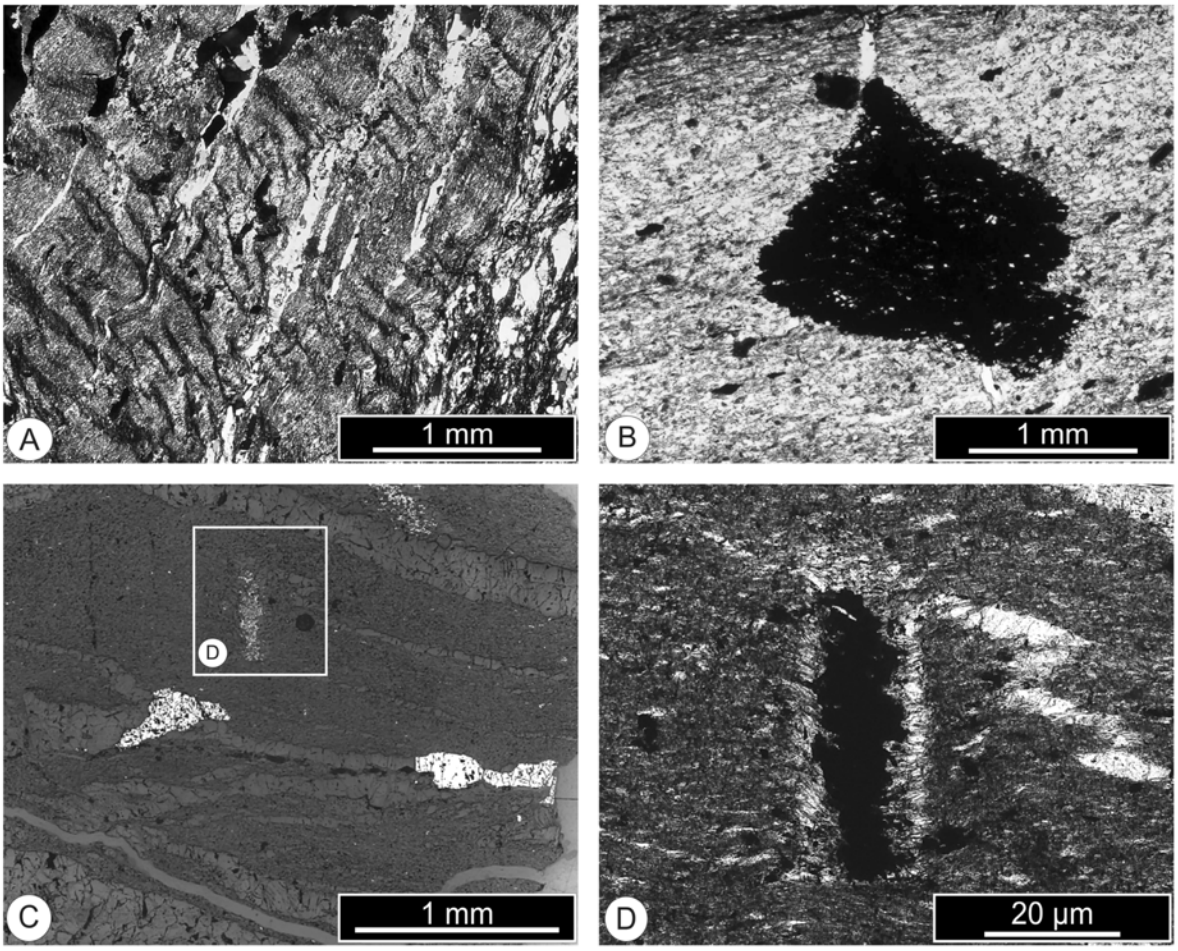

Fig. 8. Micrographs of typical phyllites in core LB-08A. a) Kink banding in chlorite-sericite layers and onset of crenulation cleavage in the competent quartz bands. Sample SR0029B0029-2-167,167. b) Aggregate of organic matter grown across the schistosity. Sample SR0053B0054-4-290,295. c, d) Different generations of ore minerals (sulfides and oxides) grown in, subparallel to, or across the well-developed schistosity. The orthogonal prism enlarged in (d) consists of organic matter finely intergrown with sulfides. Sample SR0037B0037-2-285,285. (a), (b), and (d) // nicols, (c) reflected light.

fragments in fallout suevites (Koeberl and Reimold 2005; Deutsch et al. 2005), are lacking in this core. The clasts are angular to subrounded (Fig. 10). The size of the clasts decreases from up to 1 m across in the upper part of the core (down to ~260 m) to a few millimeters in the veinlets in the lower part of core LB-08A. Sorting of clasts has not been observed.

Melt clasts are present in some allochthonous polymict breccias in core LB-08A, although the occurrence of true glass obviously is extremely rare (cf. Ferrière et al. 2007a). In our sample collection, melt lithologies are present in:

- The uppermost meters of the core, where they form clasts >3 mm across, in part vesicular and clast-laden (samples SR0001B0001-1-20,26; SR0002B0001-4-37,40; SR0002B0002-1-129,134; SR0007B0007-2-13,19; SR0008B0008-5-151,157) (cf. Fig. 4). The material is altered to different stages. The total content of such particles is low (<5 vol%); other authors (Ferrière et al. 2007a) claim the presence of <15 vol% melt lithologies at the scale of thin sections. If the matrix of some of these polymict breccias contains melt, it too is unconstrained (Fig. 10d).
- Dike breccias in the rest of the core. They contain very clast-rich, rounded, and/or elongated melt clasts <10 mm across. Occasionally the clasts are welded together and folded (samples SR0015B0015-2-192,196; SR0017B0017-2-170,176; SR0062B0064-1-78,81 [cf. Fig. 10c and 10d]; SR0062B0064-1-84,880 [Fig. 4]). The amount of such clasts may reach <15 vol% in certain areas of one thin section (sample SR0066B0068-1-80,85), yet the overall content is estimated to be distinctly less than 5 vol%. Again an extremely fine-grained matrix awaits further analyses to confirm the presence of (altered/crystallized) melt (sample SR0070B0072-2-99,105).

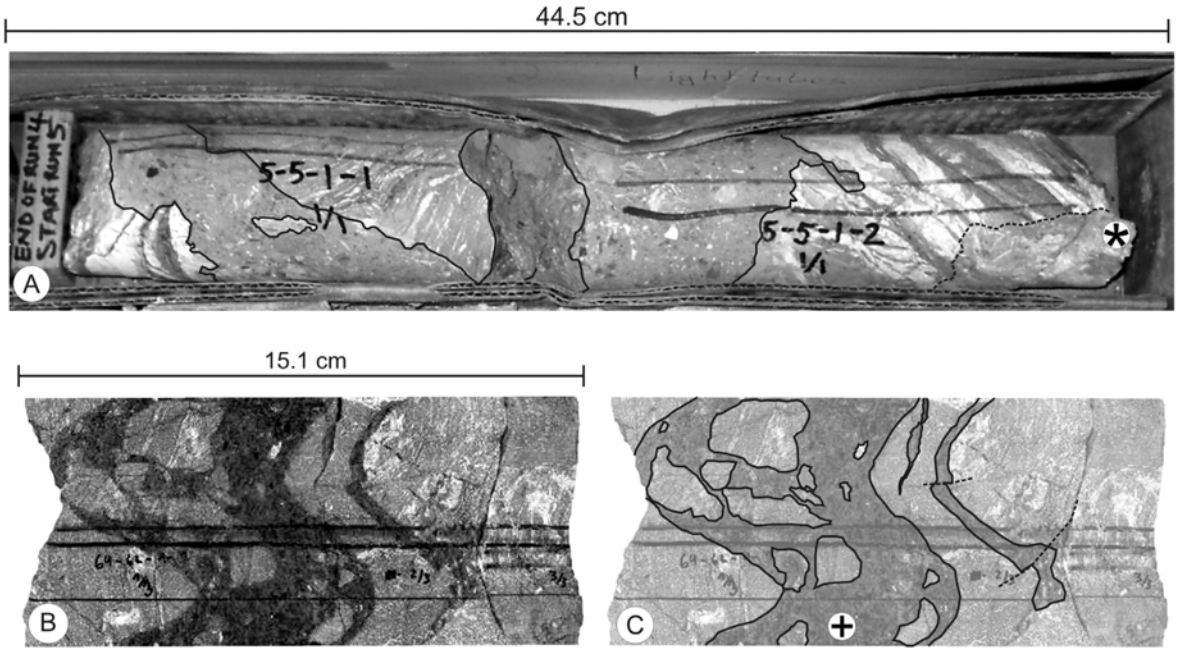

Fig. 9. Impact breccias in core LB-08A; fragments of the host rock in the dikes are enhanced. a) Polymict clastic-matrix breccia cuts into slightly distorted quartz-phyllite with alternating millimeter- to centimeter-wide quartz (in places intergrown with calcite) and sericite-graphite bands, lower right corner (✱) illustrates the onset of brecciation of the host rock. Core segment SR0005B0005-1. b) Suevitic dike (+) with clasts of quartz, meta-graywacke, phyllite, and clast-rich altered melt fragments, branching into medium-grained meta-graywacke that forms the host rock; further brecciation caused offset of the dikelets. Core segment SR0062B0064-1 (depth interval 422.21–422.74 m; core segment picture CS_R0062_BCDP-8A_3.jpg).

Concerning the number and mode of distribution of the melt clasts, these allochthonous polymict breccias fall short of being suevites, i.e., impact breccias with more than 5% or 10% cogenetic melt particles. Instead, the use of the qualifier "glass-bearing" is proposed, to prevent confusion with well-known suevites from craters like Ries in Germany, Lappajärvi in Finland, or Popigai in Russia.

(Par-)autochthonous breccias: (Par-) autochthonous breccias are monomict and comprise about 25 m of LB-08A (11.5% of the core). The autochthonous (in situ) breccias have a clastic matrix and carry only clasts of directly adjacent host rocks (Fig. 3). They often grade into intensely fractured material. There is no obvious correlation between the degrees of brecciation and U-Th-K concentrations in the borehole log (see Fig. 12 in Koeberl et al. 2007).

Shock Metamorphism

Shock effects in the target rocks of core LB-08A are widespread (Figs. 11 and 12). They are excellently developed in quartz and carbonate minerals, to a lesser degree in feldspar and sheet silicates. Quartz in meta-graywackes and phyllites displays up to four different sets of partly decorated planar deformation features (PDFs), and some grains have a "toasted" appearance (e.g., sample SR0013B0013-1-248,248). Diaplectic crystals are totally absent. A rough qualitative assessment indicates that the number of quartz crystals with shock features decreases with depth, as do the number of PDFs per grain, ending with 1 or rarely 2 sets of mostly decorated PDFs in less than 10% of the grains close to the bottom of the hole. No clear break in the intensity of shock damage has been observed, indicating a more or less continuous section. This is in accordance with observations by Elbra et al. (2007), who found no depth dependence in the variations of porosity values for target rocks. In a semiquantitative study of shock features, Ferrière et al. (2007a) document the shock attenuation in the core LB-08A in more detail. Figure 11 illustrates examples for shock features in quartz of this core; fracturing is a very common effect (Figs. 11a and 11b). Most interesting is the presence of decorated PDFs, i.e., fluid inclusions aligned along specific crystallographic planes (Figs. 11b–d). It is commonly understood that such decorated PDFs originate by post-shock annealing and alteration (e.g., Cordier and Doukhan 1989). In the case of the young Bosumtwi impact crater, annealing is estimated to be of minor importance due to the documented low peak-shock pressures, as a corollary of which annealing was only at low temperatures and for a restricted time interval (e.g., Kontny et al. 2007). The widespread presence of decorated PDFs may be related to the high fluid content in the metasediments (up to 22 wt% loss on ignition [LOI] [forthcoming data]; <13 wt% LOI in metasediments of core LB-07A) (Coney et al. 2007b) forming the target at the Bosumtwi impact site.

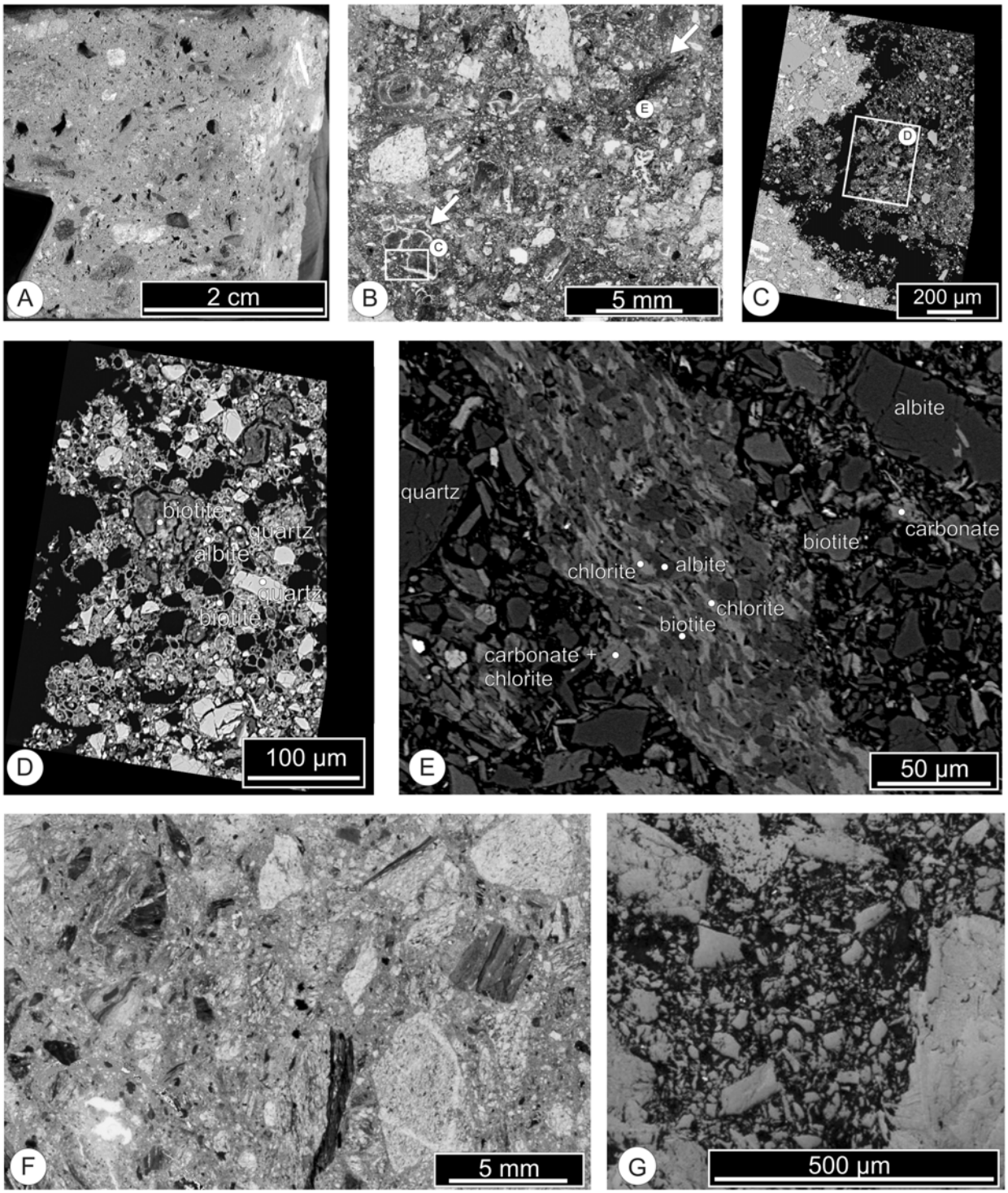

Fig. 10. Impact breccias of core LB-08A. a, b) Polymict dike breccia with foliated carbonaceous meta-graywacke as host rock; clasts show neither sorting nor specific alignment expected if a flow texture were present. b) Clasts are mostly angular; arrows mark dark fragments probably representing altered melt fragments, white rectangle and (c) and (e) mark dark brownish areas, addressed as "melted material," and are enlarged in the following SEM micrographs. Sample SR0062B0064-1-78,81. c, d) Clast-rich vesicular melted domain. e) This area turned out to consist of mineral clasts and a fine-grained slate fragment. f) Polymict lithic breccia with angular fragments of meta-graywacke, banded slates and phyllites, partly rich in organic matter; melt particles, if present, are not obvious. Sample SR0008B0008-5-151,157. g) Polymict lithic breccia capping the uplifted target; all clasts down to the micrometer scale are angular. The nature of the matrix (dark) is unconstrained yet may contain melt material. Sample SR0001B0001-1-20,26. Fragments show angular shapes. a) Macro photo of core pieces. f) Macro photo of thin section. b, g) Micrographs with (b) // nicols and (g) in reflected light.

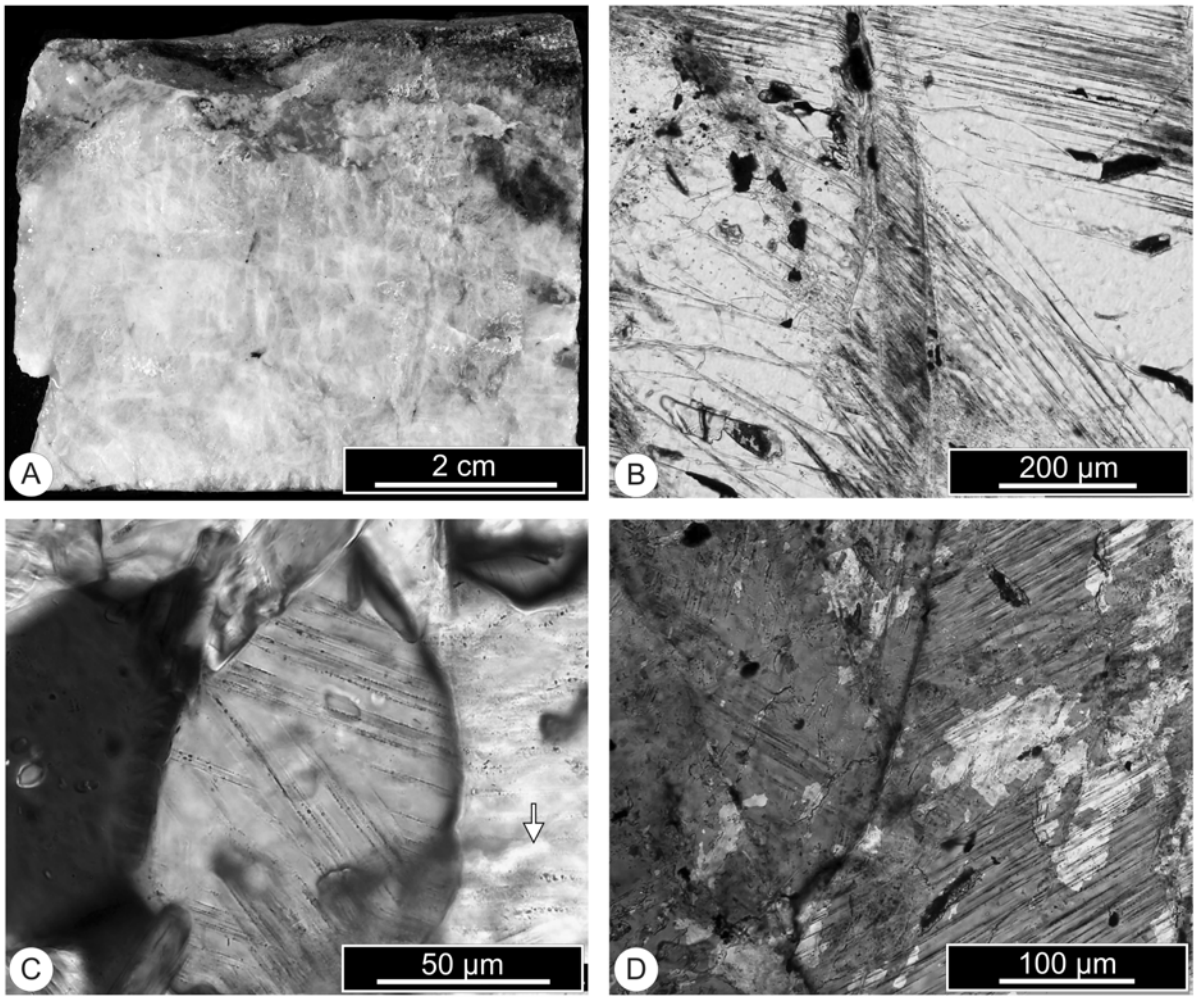

Fig. 11. Quartz in lithologies of core LB-08A. a, b) A cut piece of an ~25 cm thick quartz vein. Sample SR0065B0067-3-145,150. b) Two sets of partly decorated PDFs cross over two N-S trending fractures. c) A quartz grain with two sets of decorated PDFs in contact with a quartz grain containing decorated Böhm lamellae (arrow in lower left corner), phyllite. Sample SR0008B0008-5-151,157. d) Quartz grains with up to three sets of partly decorated PDFs, crossing over grain boundaries, monomict meta-graywacke breccia. Sample SR0013B0013-1-248,248. (b) //, (c) and (d) + nicols.

Nearly all carbonate minerals (mostly calcite) display a number of impressive shock effects (Fig. 12): up to 3 sets of polysynthetic twins penetrating each other (Figs. 12b and 12c) occur. Some grains show planar fractures (PFs) with several crystallographic orientations (Fig. 12c). The presence of these effects documents unambiguously that carbonates belong predominately to a pre-shock mineral assemblage. Some carbonate veinlets and stockwork, however, may be related to post-impact processes (cf. Ferrière et al. 2007a). Regarding the shock pressure necessary to yield the features observed in calcite, only a qualitative assessment (e.g., Langenhorst and Deutsch 1998) and some experimental data are available (Langenhorst et al. 2002). A systematic classification of shock metamorphic features in carbonate minerals, especially in calcareous (meta-)graywackes, is lacking so far.

Sheet silicates show kinking, yet this effect is rather restricted in its distribution; ore minerals frequently display brecciation. In general, the number and type of shock effects is concentrated in the easily compressible minerals; phyllites therefore display fewer shock features than the meta-graywackes at the microscopic scale. The observed sequence of effects is in line with generally accepted schemes of shock metamorphism (e.g., Langenhorst and Deutsch 1994, 1998). Interesting to note is the total lack of diaplectic quartz crystals in target rocks (in contrast to the impact breccias), which constrain the maximum shock pressure in the uplifted target lithologies to less than 26 GPa (e.g., Langenhorst and Deutsch 1994).

In the breccias, shock effects are identical to those occurring in the target lithologies except for the rare presence of the above discussed melt particles in the suevites, and the even rarer occurrence of diaplectic quartz crystals in the uppermost part of the section (cf. Ferrière et al. 2007a).

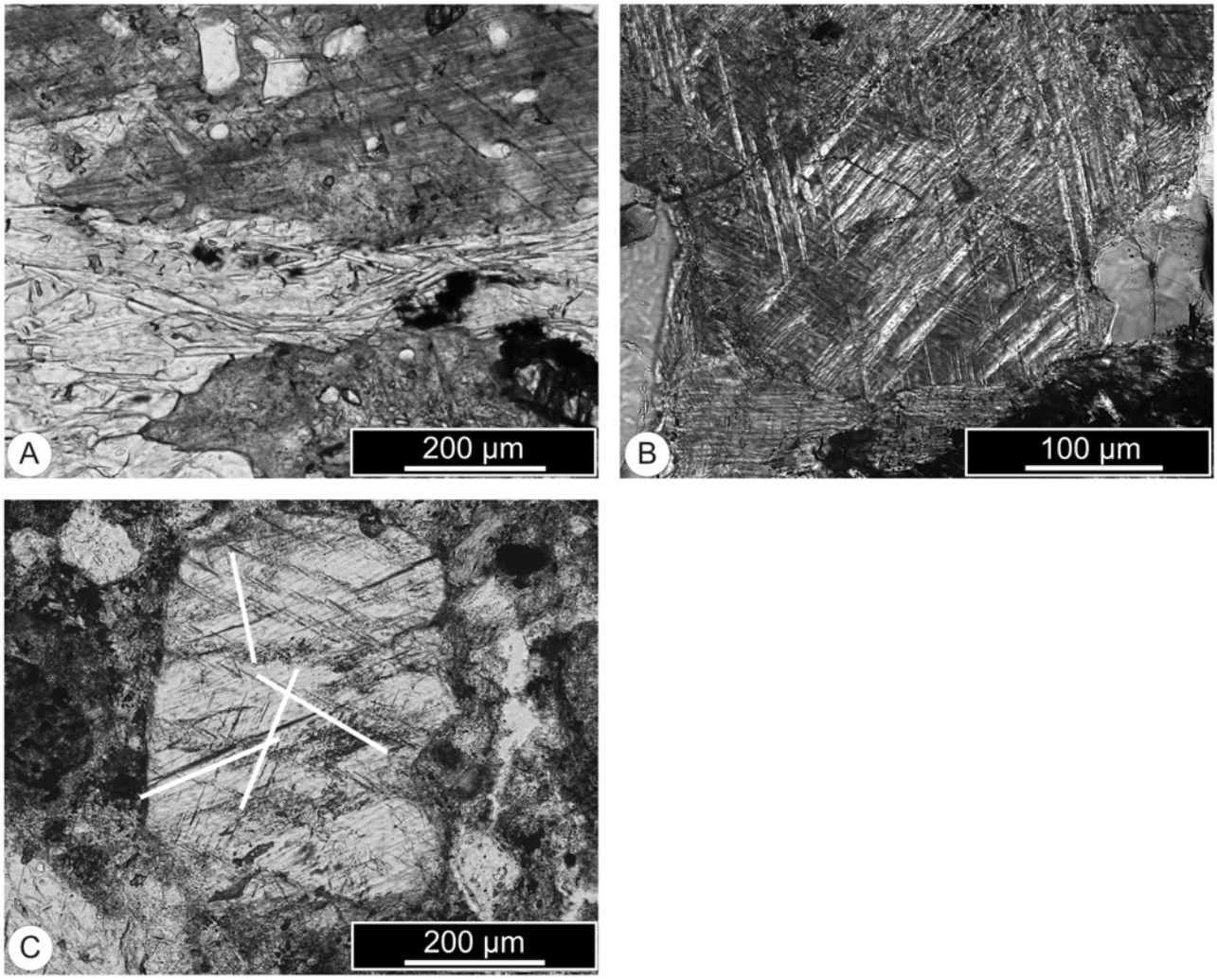

Fig. 12. Micrographs of carbonate minerals in lithologies of core LB-08A. a) The pre-impact assemblage of this calcite-rich quartz-phyllite (host rock to a suevitic dike breccia) consists of closely intergrown calcite, quartz, chlorite, and sericite. Calcite crystals show one set of polysynthetic twins, and two sets of PFs. No shock effects are present in the other minerals in this part of the thin section. Quartz crystals of this sample rarely display PFs. Sample SR0062B0064-1-96,100. b) Three set of polysynthetic twins in a calcite crystal of a meta-graywacke. Sample SR0044B0044-3-105,105. c) One set of polysynthetic twins and four sets of PFs in a calcite crystal, clast (~20 mm across) of carbonaceous meta-graywacke in a melt-rich suevitic dike breccia. Sample SR0062B0064-1-84,88. (a) //, (b) and (c) + nicols.

Litho-Units

While the situation is complicated in detail (cf. Fig. 3; http://www.icdp-online.de/contenido/icdp/upload/pdf/lake_bosumtwi/secure/lithounits_8A.txt), for the purpose of modeling a more simplified concept can be used. From 235 m down to about 260 m, the section is composed of a melt-bearing allochthonous, polymict, and mostly clast-supported breccia. It is not yet clear if the meter-long intervals of quartz-phyllite and meta-graywacke are just large fragments (the preferred interpretation) or if they are true intercalations in tongues of breccia. Below this polymict breccia, down to about 418 m, the section consists of a rather uniform unit of meta-graywacke alternating with phyllite to slate; few breccia bodies and rare dikes are present. It is yet not clear if this unit represents one large yet broken block of target material, or several smaller blocks thrusted and displaced along impact-induced faults. The lowermost part of the section is characterized by the presence of melt-bearing breccia dikes in country rocks identical to those occurring above. Transport distance in these dikes is unconstrained but the melt particles clearly have originated far from their present location.

Structural Elements

Macroscopically observable folding is occasionally present, as illustrated in the most spectacular example: a core segment from LB-07A (Fig. 13). In general, foliation cuts bedding; in places both these textural elements cannot be discerned. Meta-graywackes and phyllites dip from 10° up to about 55° with respect to the core axis (Fig. 3); abruptly changing dip angles occur just in core intervals that comprise

(par-) autochthonous breccias. This observation is compatible with either i) impact-induced or ii) drilling-induced "shattering." Taking observations from the Vorotilovo deep drilling at the Puchez-Katunki structure into account (Masaitis and Pevzner 1999), strongly shattered intervals confine single blocks in the uplift of this crater. If this is also the case in the uplift at Bosumtwi, the block size there ranges from <20 m up to about 50 m (cf. Fig. 3).

Fracturing

The cored material contains two types of fractures, being either pre-impact in age or impact-related. For the former, the older generation of fractures postdates regional metamorphism and is accompanied by stockworks and stringers of quartz and calcite (see above). Often two sets of crossing fractures occur; these types of fracture are observed in all parts of the core except for about the uppermost 30 m. Below ~415 m in depth, nearly vertical, partly open fractures coated with chlorite occur. Calcite and fine-grained chlorite flakes occasionally decorate the open fractures; growth of these crystals is assessed as a pre-impact process. At the microscopic scale, sulfides form veinlets, which are ruptured in samples with fractures of generation (the latter type of fracture). Although these fractures are considered to be a pre-impact phenomenon, the opening represents an effect caused by dilatation after pressure release.

For the latter type of fracture, compared to cores from other impact structures (e.g., Ries, Pohl et al. 1977), parts of LB-08A contain such a high number of fractures that most of the rocks are extremely fragile. The material disintegrated during handling (e.g., cutting) into rubble or irregular pieces of up to a few centimeters in size (Fig. 14a). Unless disintegrated, the single pieces are displaced and/or distorted to each other only by a few degrees, and no matrix of pulverized rocks in between the respective pieces has been observed. It cannot be totally excluded that this feature is partly an effect of drilling-induced stress (see below). Approximately 90 m of the cored material (~41% of the core) is characterized by this type of fracturing (cf. Deutsch et al. 2006) (Fig. 3). If, however, this fracturing throughout combined with cracks at all scales is due to the impact event, we should expect elastic wave velocities P and S to be substantially reduced.

Disking

Approximately 89 m of the LB-08A cores (~40% of the core) display severe disking with a thickness of individual disks ranging from 1 to ~5 cm (Fig. 14b). Prominent intervals with disking occur at 265–280 m, 298–310 m, 318–336 m, 338–363 m, 371–384 m, and 387–391 m in depth. This phenomenon is well known from drilling and tunnel construction in mountain regions and deep mining operations (e.g., Brown and Trollope 1967), and reflects release from high lithostatic pressure. In the case of Bosumtwi, however, we exclude this process as the reason for the disking, since the overload by post-impact sediments is insufficient to impose enough lithostatic pressure. An alternative explanation as cause for the disking is the application of pressure that is too high for the drilling bits.

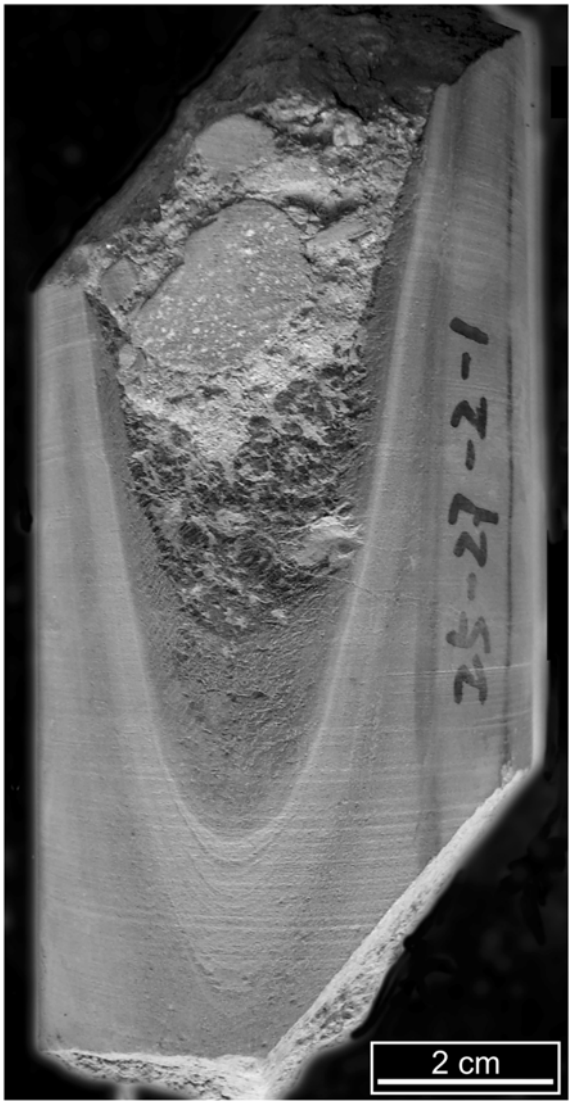

Fig. 13. Folding in light, fine-grained meta-graywacke; core LB-07A, depth of about 411 m.

SHOCK RECOVERY EXPERIMENTS

Shock barometry via petrographic analysis helps to understand cratering mechanics, particularly mass movements in the central uplift, including its collapse in the late stage of cratering. Shock pressures recorded in uplifted target lithologies of the central uplift may exceed 45 GPa, e.g., in the Vorotilovo core drilled into the center of the Puchezh-Katunki structure, Russia (Masaitis and Pevzner 1999). In addition, allochthonous breccia bodies in the uplift

Fig. 14. Fracturing (a) and disking (b) in core LB-08A. a) Rows one and five of box B0067 comprise intervals with rubble only ("fracturing of type 5" in the profile of Fig. 3). Note the sharp boundary of apparently coherent material that breaks to pieces if even only slight pressure is applied. The fracturing is due to impact-induced weakening of the target rocks. b) Meta-graywackes in row three of box B0011 display severe disking in individual disks with a thickness ranging from 1 to ~5 cm. This type of disintegration is assumed to be caused by drilling.

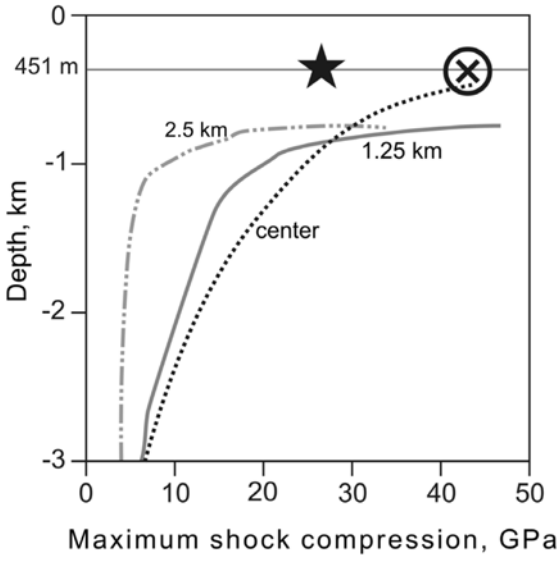

Fig. 15. Depth-shock pressure graph for three modeled drilling locations at Lake Bosumtwi, at the crater center (dotted), 1.25 (line), and 2.5 km (chain dotted) off the center. The horizontal line corresponds to the final depth of well LB-08A, the star to the maximum shock pressure derived from petrographic analysis of the target rocks, the cross to the maximum pressure derived from the model (i.e., <45 GPa). Modified after Artemieva et al. (2004).

may contain impact-melt lithologies as either matrix or clasts, and even layers of impact-melt rocks (tagamites) have been observed (e.g., Masaitis and Pevzner 1999). Maximum shock pressure recorded in the drilled uplifted basement at the Ries and Rochechouart are between 28 and 30 GPa (e.g., Engelhardt and Graup 1977; Lambert 1977); at the eroded Slate Islands and Charlevoix impact structures Robertson and Grieve (1977) report quartz with shock effects typical for pressures of up to 23 GPa. In the Ries crater, however, a much larger amount of suevites has been determined inside the crater, and shock levels of 35–40 GPa are recorded in rocks forming the ring uplift (Engelhard and Graup 1977). At this dynamic pressure quartz is totally converted to diaplectic glass in single crystal shock recovery experiments (Langenhorst and Deutsch 1994) and naturally shocked crystalline rocks (e.g., Langenhorst and Deutsch 1998). In contrast, SiO_2 glass and coesite already occur in the pressure interval of 5 to ~13 GPa if the target is porous, such as the Coconino sandstone at Barringer crater, Arizona, USA (e.g., Kieffer et al. 1977). Shock barometry in calcite, especially at rather low dynamic pressures, is still in its infancy (e.g., Langenhorst and Deutsch 1998).

Taking all the facts together, the target lithologies and various clastic-matrix breccias encountered in well LB-08A in the central uplift of the Lake Bosumtwi impact structure

Table 1. Parameters for shock recovery experiments.

Experiment number, sample ∅ = 10 mm, *d* = 0.5 mm	*P* (GPa)	*d* flyer plate (mm)	*d* driver plate container (mm)	High explosive
VZ-#10.929 EP7: K/T boundary, El Peñon, northeast Mexico	34	4	9.5	Composition B
VZ-#10.930 VÑ2: Vañes Formation, Westphalian, Cantabrian Mountains, Spain	39.5	4	3.2	Composition B

P = calculated equilibrium pressure, *d* = thickness, ∅ = diameter, composition B = castable high explosive made of 60% hexogen and 40% TNT mixed with wax.

yielded a picture different from that observed in other terrestrial impact structures, and quite different from that expected on the basis of modeling. Shock levels recorded in the carbonaceous meta-graywackes, phyllites, and slates amount to only about 26 GPa, which is much less than expected by the interpretation of geophysical data (e.g., Karp et al. 2002) and numerical modeling (Artemieva et al. 2004). As illustrated in Fig. 15, numerical modeling predicts the presence of a 100–200 m thick layer of melt lithologies topping the central uplift and its flank, and a shock level in excess of 40 GPa in the uppermost portion of the uplifted target rocks. Melt lithologies, however, are nearly absent in core LB-08A, except for the rare millimeter-size clasts of altered impact-melted material in polymict breccias. In addition, diaplectic glasses occur very rarely (cf. Ferrière et al. 2007a). It is yet unconstrained whether these strange features are due to a specific shock behavior of the rather soft, porous, and fluid-rich metasediments (see above) or are related to the as-yet undefined parameters of the cratering event (e.g., obliquity of the impact).

Experimental Approach

To tackle the problem of the "surprisingly low shock metamorphic overprint," shock recovery experiments were carried out with a conventional setup (Langenhorst and Deutsch 1994) at 34 and 39.5 GPa (see Table 1 for details). This setup consists of the sample disk embedded in an ARMCO steel container as momentum trap, and a high-explosive-driven flyer plate. The 0.5 mm thick sample disks, polished on both sides, were carbonaceous graywackes of a composition similar to the corresponding target lithology at the Lake Bosumtwi crater; i.e., a graywacke containing 20 vol% calcite (courtesy H. Bahlburg, Münster).

Results

Both experimentally shocked carbonaceous graywackes display intense fracturing, although the respective original texture is fully preserved (Fig. 16). At both shock levels, quartz grains display planar elements, and most of the quartz is transformed to diaplectic crystals (Figs. 16b and 16c). Calcite shows multiple shock-induced polysynthetic twins (Figs. 16c and 16d) as well as mosaicism and PFs. These observed shock effects compare well with data from single crystal shock experiments (Langenhorst and Deutsch 1994; Langenhorst et al. 2002), and the generally accepted shock wave barometry (e.g., French 1998). Moreover, these results indicate that the shock behavior of quartz in carbonaceous graywackes is not completely different than that of single crystal quartz crystals or quartz in quartz-rich meta-sandstones.

DISCUSSION

Both experimentally shocked graywackes contain diaplectic quartz crystals. Suevite from locations outside the rim of the Bosumtwi crater (Boamah and Koeberl 2002, 2006; Deutsch et al. 2005; Koeberl and Reimold 2005) contain diaplectic crystals and coesite, as well as true melt glasses. In contrast to this ejecta, lithologies cored in LB-08A seem to nearly totally lack such highly shocked material. The lithological characterization of the core LB-07A in the annular moat (Coney et al. 2007a) also points to only minor amounts of impact-melted materials there. Clasts of melt lithologies in the suevite of core LB-07A amount to between 1.6–6.8 vol%, and diaplectic quartz glass occurs rather rarely (observed maximum in a thin section is 3.7 vol% [Coney et al. 2007a]). These authors state that the bulk of suevite in LB-07A appears to have been derived from the <35 GPa shock zone of the transient crater. Taking these observations together, a specific shock behavior of the soft target material (carbonaceous graywackes, phyllites, slates, and shales) is rather unlikely as the prime reason for the generally low shock levels recorded in different lithologies inside the Lake Bosumtwi impact crater. Rather, this surprising feature may be related to an oblique impact.

Using refined numerical modeling, Artemieva (2007) discusses various reasons behind the melt deficiency observed in the two "hard-rock" drill cores LB-07A and LB-08A of the ICDP Lake Bosumtwi project. Specific impact scenarios such as a low impact velocity and/or low impact angle may help to explain the distribution of melt lithologies in and around the Bosumtwi impact structure. In all calculated models, the rock column in the center of the crater, corresponding more or less to core LB-08A in the central

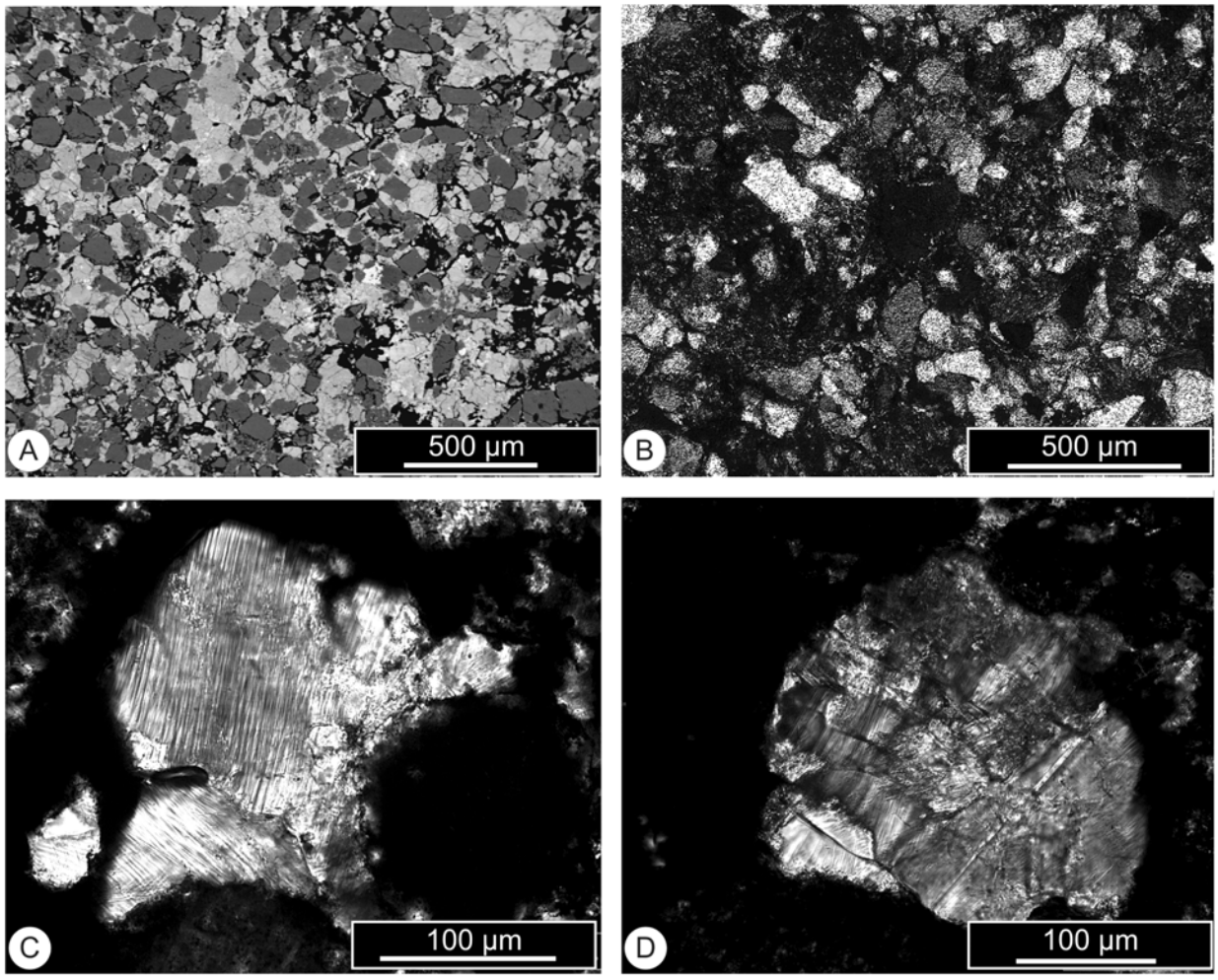

Fig. 16. Micrographs of the carbonaceous graywacke VÑ2 shocked experimentally at a calculated equilibrium pressure of 39.5 GPa (cf. Table 1). a) SEM overview. b) Quartz is transformed to diaplectic crystals. c, d) Calcite displaying (c) mechanical twinning and (d) twinning, planar elements, and mosaicism. b–d) + nicols.

uplift, is shocked to between 10 and 37 GPa. At the latter dynamic pressure, all quartz should be transformed to diaplectic glass (Langenhorst and Deutsch 1994). This is not the case in any sample, and all authors state that diaplectic quartz glass occurs quite rarely (this work; Coney et al. 2007a; Ferrière et al. 2007a). One major discrepancy between the modeled results published by Artemieva et al. (2004) and the reality in the Bosumtwi case is that "granite" was used as target material in the models. Mechanically, this material behaves quite differently than the meta-graywackes and phyllites encountered in the wells LB-07A and LB-08A. The respective consequences of specific target properties such as modal composition, high porosity, and high content of volatiles on shock effects in the named metasediments are, however, either poorly constrained or not explored yet. For example, the average porosity of the metasedimentary target rocks is less than 10% (Elbra et al. 2007). Such knowledge, however, seems to be necessary to better understand the observational data, namely the relatively low shock-metamorphic overprint of the metasediments in the central uplift. To overcome the obvious deficiencies in knowledge, we need both more refined numerical modeling as well as shock recovery experiments with appropriate materials in the pressure range of interest.

The results of various drilling projects in impact structures have contributed significantly to enhancing the understanding of various aspects of cratering. Excellently documented examples are Ames, Oklahoma, USA (Johnson and Campbell 1997); Chesapeake Bay, USA (Poag et al. 2004; Gohn et al. 2006); Chicxulub, Mexico (papers in *Meteoritics & Planetary Science* vol. 39, issues 6 and 7, 2004); Manson, Iowa, USA (Koeberl and Anderson 1996); Forschungsbohrung Nördlingen; Ries impact structure (papers in *Geologica Bavarica* vols. 72 and 75); Puchez-Katunki, Russia (Masaitis and Pevzner 1999); and Siljan, Sweden (papers in Bodén and Eriksson 1988). The first scientific results of the ICDP Lake Bosumtwi Project document impressively that only drilling yields the basic data necessary to better understand cratering and refine cratering models.

Acknowledgments–Drilling was funded by ICDP, the U.S. NSF, the Austrian FWF, the Canadian NSERC, and the Austrian Academy of Sciences. Drilling operations were performed by DOSECC. Local help by the Geological Survey Department (Accra) and KNUST (Kumasi), Ghana, were invaluable. This study was supported by German Science Foundation [DFG] grant De 401/19. We appreciate the support, help, and hospitality of the ICDP Operational Support Group, Potsdam (R. Conze, U. Harms, J. Kück, Th. Wörl), scientific advice by U. Hornemann (EMI, Freiburg i. Br.), and skillful technical assistance by F. Bartschat, M. Feldhaus, U. Heitmann, and T. Grund (Münster). Intense discussions with N. Artemieva (Moscow, Toronto), L. Ferrière, C. Koeberl (Vienna), W. U. Reimold, K. Wünnemann (Berlin), B. Milkereit (Toronto), A. Kontny (Heidelberg), K. Heide, F. Langenhorst, B. Kreher-Hartmann (Jena), and L. Coney (Johannesburg) helped in understanding the in part puzzling observations. L. Ferrière and T. Kenkmann are thanked for critical and constructive reviews. This work forms part of the Ph.D. thesis of S. Luetke.

Editorial Handling—Dr. Christian Koeberl

REFERENCES

Artemieva N. 2007. Possible reasons of shock melt deficiency in the Bosumtwi drill cores. *Meteoritics & Planetary Science* 42. This issue.

Artemieva N., Karp T., and Milkereit B. 2004. Investigating the Lake Bosumtwi impact structure: Insight from numerical modeling. *Geochemistry Geophysics Geosystems* 5, doi:10.1029/2004GC000733.

Boamah D. and Koeberl C. 2002. Geochemistry of soils from the Bosumtwi impact structure, Ghana, and relationship to radiometric airborne geophysical data. In *Meteorite impacts in Precambrian shields,* edited by Plado J. and Pesonen L. Impact Studies, vol. 2. Heidelberg-Berlin: Springer. pp. 211–255.

Boamah D. and Koeberl C. 2006. Petrographic studies of "fallout" suevite from outside the Bosumtwi impact structure, Ghana. *Meteoritics & Planetary Science* 41:1761–1774.

Bodén A. and Eriksson K. G., editors. 1988. *The deep gas drilling in the Siljan impact structure, Sweden, and astroblemes.* Deep drilling in crystalline bedrock, vol. 1. Berlin: Springer. 364 p.

Brown E. T. and Trollope D. H. 1967. The failure of linear brittle materials under effective tensile stress. *Felsmechanik und Ingenieurgeologie* 5:329–241.

Coney L., Gibson R. L., Reimold W. U., and Koeberl C. 2007a. Lithostratigraphic and petrographic analysis of ICDP drill core LB-07A, Bosumtwi impact structure, Ghana. *Meteoritics & Planetary Science* 42. This issue.

Coney L., Reimold W. U., Gibson R. L., and Koeberl C. 2007b. Geochemistry of impactites and basement lithologies from ICDP borehole LB-07A, Bosumtwi impact structure, Ghana. *Meteoritics & Planetary Science* 42. This issue.

Cordier P. M. and Doukhan J. C. 1989. Water solubility in quartz and its influence on ductility. *European Journal of Mineralogy* 1: 221–237.

Danuor S. 2004. Geophysical investigations of the Bosumtwi impact crater and comparison with terrestrial meteorite craters of similar age and size. Ph.D thesis, Kwame Nkrumah University of Science and Technology, Kumasi, Ghana.

Deutsch A., Heinrich V., and Luetke S. 2006. The Lake Bosumtwi impact crater drilling project (BCDP): Lithological profile of well hole BCDP-8A (abstract #1292). 37th Lunar and Planetary Science Conference. CD-ROM.

Deutsch A., Langenhorst F., Heide K., Bläss U., and Sokol A. 2005. Unusual staurolite-rich target rocks and glass-rich suevite at the Lake Bosumtwi impact structure, Ghana, West Africa (abstract). *Meteoritics & Planetary Science* 40:A40.

Engelhardt W. von and Graup G. 1977. Stosswellenmetamorphose im Kristallin der Forschungsbohrung Nördlingen 1973. *Geologica Bavarica* 55:255–272.

Elbra T., Kontny A., Pesonen L. J., Schleifer N., and Schell C. 2007. Petrophysical and paleomagnetic data of drill cores from the Bosumtwi impact structure, Ghana. *Meteoritics & Planetary Science* 42. This issue.

Ferrière L., Koeberl C., and Reimold W. U. 2007a. Drill core LB-08A, Bosumtwi impact structure, Ghana: Petrographic and shock metamorphic studies of material from the central uplift. *Meteoritics & Planetary Science* 42. This issue.

Ferrière L., Koeberl C., Reimold W. U., and Mader D. 2007b. Drill core LB-08A, Bosumtwi impact structure, Ghana: Geochemistry of fallback breccia and basement samples from the central uplift. *Meteoritics & Planetary Science* 42. This issue.

French B. M. 1998. *Traces of catastrophe: A handbook of shock-metamorphic effects in terrestrial meteorite impact structures.* Houston, Texas: Lunar and Planetary Science Institute. 120 p.

Glass B. P., Kent D. V., Schneider D. A., and Tauxe L. 1991. Ivory Coast microtektite strewn field: Description and relation to the Jaramillo geomagnetic event. *Earth and Planetary Science Letters* 107:182–196.

Gohn G. P., Kent D. V., Schneider D. A., and Tauxe L. 2006. Ivory Coast microtektite strewn field: Description and relation to the Jaramillo geomagnetic event. *Eos Transactions* 107:182–196.

Johnson K. S. and Campbell J. A., editors. 1997. Ames structure in northwest Oklahoma and similar features: Origin and petroleum production. Oklahoma Geological Survey Circular #100. 396 p.

Jones W. B., Bacon M., and Hastings D. A. 1981. The Lake Bosumtwi impact crater, Ghana. *Geological Society of America Bulletin* 92:342–349.

Karp T., Milkereit B., Janle J., Danuor S. K., Pohl J., Berckhemer H., and Scholz C. A. 2002. Seismic investigation of the Lake Bosumtwi impact crater: Preliminary results. *Planetary Space Science* 50:735–743.

Kieffer S. W., Phakey P. P., and Christie J. M. 1976. Shock processes in porous quartzite: Transmission electron microscope observations and theory. *Contributions to Mineralogy and Petrology* 59:41–93.

Koeberl C. and Anderson R. R.1996. *The Manson impact structure, Iowa: Anatomy of an impact crater.* GSA Special Paper #302. Boulder, Colorado: Geological Society of America. 468 p.

Koeberl C. and Reimold W. U. 2005. Bosumtwi impact crater, Ghana (West Africa): An updated and revised geological map, with explanations. *Jahrbuch der Geologischen Bundesanstalt Wien (Yearbook of the Austrian Geological Survey)* 145:31–70 (+1 map, 1:50,000).

Koeberl C., Bottomley R. J., Glass B. P., and Storzer D. 1997. Geochemistry and age of Ivory Coast tektites and microtektites. *Geochimica et Cosmochimica Acta* 61:1745–1772.

Koeberl C., Reimold W. U., Blum J. D., and Chamberlain C. P. 1998. Petrology and geochemistry of target rocks from the Bosumtwi impact structure, Ghana, and comparison with Ivory Coast tektites. *Geochimica et Cosmochimica Acta* 62:2179–2196.

Koeberl C., Milkereit B., Overpeck J. T., Scholz C. A., Amoako

P. Y O., Boamah D., Danuor S., Karp T., Kueck J., Hecky R. E., King J. W., and Peck J. A. 2007. An international and multidisciplinary drilling project into a young complex impact structure: The 2004 ICDP Bosumtwi Crater Drilling Project—An overview. *Meteoritics & Planetary Science* 42. This issue.

Kontny A., Elbra T., Just J., Pesonen L. J., Schleicher A., and Zolk J. 2007. Petrography and shock-related remagnetization of pyrrhotite in drill cores from the Bosumtwi Impact Crater Drilling Project, Ghana. *Meteoritics & Planetary Science* 42. This issue.

Lambert P. 1977. The Rochechouart crater: Shock zoning study. *Earth and Planetary Science Letters* 35:258–268.

Langenhorst F. and Deutsch A. 1994. Shock experiments on pre-heated α- and β-quartz: I. Optical and density data. *Earth and Planetary Science Letters* 125:407–420.

Langenhorst F. and Deutsch A. 1998. Mineralogy of astroblemes—Terrestrial impact craters. In *Advanced mineralogy III, mineral matter in space, mantle, ocean floor, biosphere, environmental management, jewelry,* edited by Marfunin A. S. Berlin: Springer. pp. 95–11.

Langenhorst F., Boustie M., Deutsch A., Hornemann U., Matignon Ch., Migault A., and Romain J. P. 2002. Experimental techniques for the simulation of shock metamorphism: A case study on calcite. In *High-pressure shock compression of solids V—Shock chemistry and meteoritic applications,* edited by Davison L., Horie Y., and Sekine T. Berlin: Springer. pp. 1–27.

Masaitis V. L. and Pevzner L. A. 1999. *Deep drilling in the Puchezh-Katunki impact structure.* Saint Petersburg: VSEGEI Press. 392 p.

Moon P. A. and Mason D. 1967. The geology of 1/4° field sheets nos. 129 and 131, Bompata S.W. and N.W. *Ghana Geological Survey Bulletin* 31:1–51.

Morrow J. 2007. Shock-metamorphic petrography and microRaman spectroscopy of quartz in upper impactite interval, ICDP drill core LB-07A, Bosumtwi impact crater, Ghana. *Meteoritics & Planetary Science* 42. This issue.

Pesonen L. J., Koeberl C., and Hautaniemi H. 2003. Airborne geophysical survey of the Lake Bosumtwi meteorite impact structure (southern Ghana)—Geophysical maps with descriptions. *Jahrbuch der Geologischen Bundesanstalt, Vienna (Yearbook of the Austrian Geological Survey)* 143:581–604.

Plado J., Pesonen L. J., Koeberl C., and Elo S. 2000. The Bosumtwi meteorite impact structure, Ghana: A magnetic model. *Meteoritics & Planetary Science* 35:723–732.

Poag C. W., Koeberl C., and Reimold W. U. 2004. *The Chesapeake Bay crater.* Berlin: Springer. 522 p.

Pohl J., Stöffler D., Gall H., and Ernstson K. 1977. The Ries impact crater. In *Impact and explosion cratering,* edited by Roddy D. J., Pepin R. O., and Merrill R. B. New York: Pergamon Press. pp. 343–404.

Reimold W. U., Brandt D., and Koeberl C. 1998. Detailed structural analysis of the rim of a large, complex impact crater: Bosumtwi crater, Ghana. *Geology* 26:543–546.

Robertson P. B. and Grieve R. A. F. 1977. Shock attenuation at terrestrial impact structures. In *Impact and explosion cratering,* edited by Roddy D. J., Pepin R. O., and Merrill R. B. New York: Pergamon Press. pp. 687–7021.

Rock-Color Chart Committee. 1979. Rock-color chart. Boulder, Colorado: Geological Society of America.

Scholz C. A., Karp T., Brooks K. M., Milkereit B., Amoako P. Y. O., and Arko J. A. 2002. Pronounced central uplift identified in the Bosumtwi impact structure, Ghana, using multichannel seismic reflection data. *Geology* 30:939–942.

Ugalde H. 2006. Geophysical signature of small to midsize terrestrial impact structures. Ph.D thesis, University of Toronto, Toronto, Canada.

Ugalde H., Danuor S. K., and Milkereit B. 2007. Integrated 3-D model from gravity and petrophysical data at the Bosumtwi, impact structure, Ghana. *Meteoritics & Planetary Science* 42. This issue.

Wagner R., Reimold W. U., and Brandt D. 2002. Bosumtwi impact crater, Ghana: A remote sensing investigation. In *Meteorite impacts in Precambrian shields,* edited by Plado J. and Pesonen L. Heidelberg: Springer. pp. 189–210.